



OPEN ACCESS

EDITED BY

Lianjie Huang,
Los Alamos National Laboratory (DOE),
United States

REVIEWED BY

Vlad Constantin Manea,
National Autonomous University of
Mexico, Mexico
Yong Zheng,
China University of Geosciences Wuhan,
China

*CORRESPONDENCE

Vivek Kumar,
✉ vivek.seismology@gmail.com

RECEIVED 20 July 2023

ACCEPTED 31 October 2023

PUBLISHED 24 November 2023

CITATION

Kumar V (2023), Preserved and modified arc crust beneath the Kohistan-Ladakh arc in the western Himalaya-Karakoram region: evidence from ambient noise and earthquake data.

Front. Earth Sci. 11:1264415.

doi: 10.3389/feart.2023.1264415

COPYRIGHT

© 2023 Kumar. This is an open-access article distributed under the terms of the [Creative Commons Attribution License \(CC BY\)](https://creativecommons.org/licenses/by/4.0/). The use, distribution or reproduction in other forums is permitted, provided the original author(s) and the copyright owner(s) are credited and that the original publication in this journal is cited, in accordance with accepted academic practice. No use, distribution or reproduction is permitted which does not comply with these terms.

Preserved and modified arc crust beneath the Kohistan-Ladakh arc in the western Himalaya-Karakoram region: evidence from ambient noise and earthquake data

Vivek Kumar*

Department of Earth and Climate Science, Indian Institute of Science Education and Research Pune, Pune, India

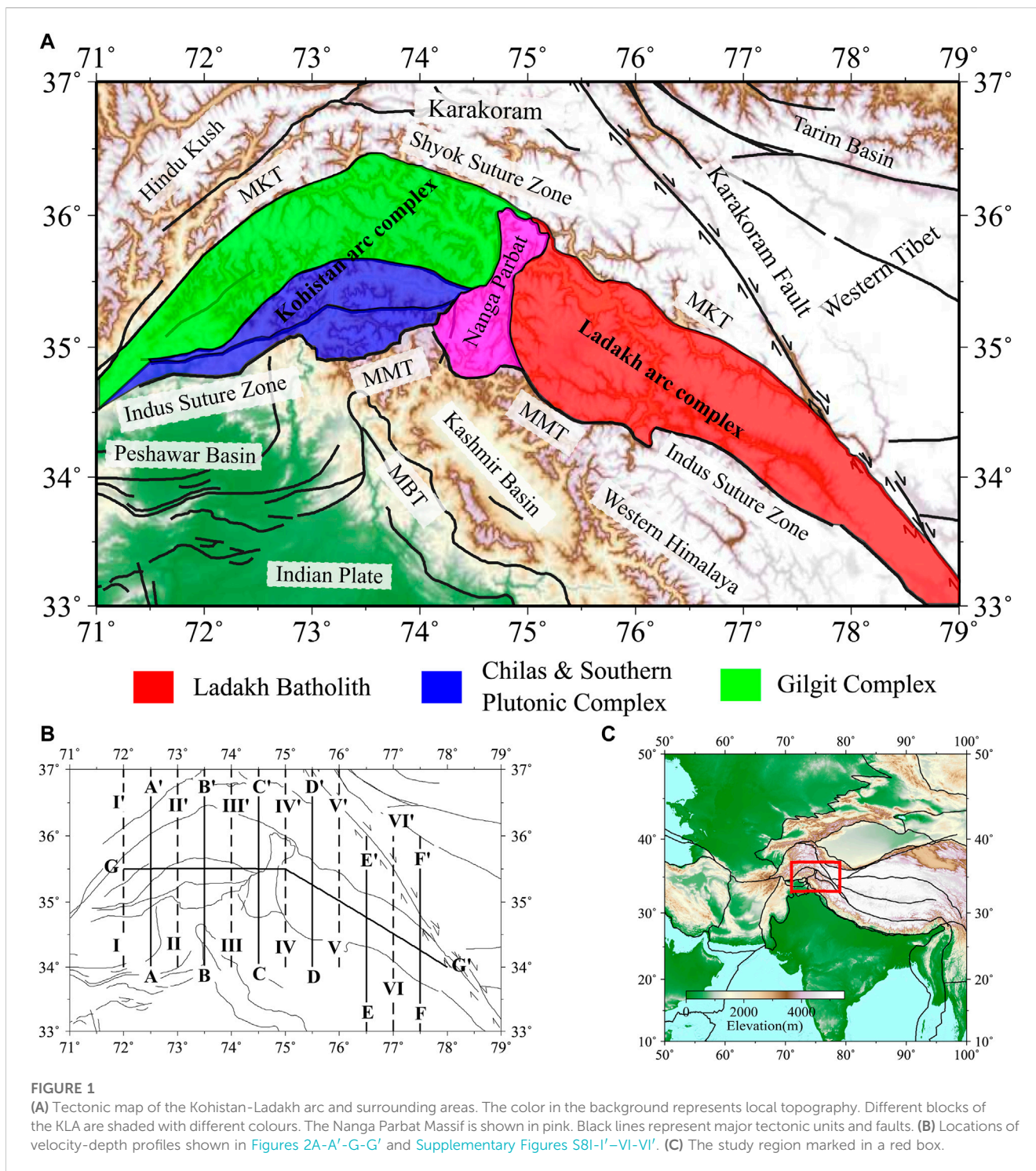
This study uses ambient noise and earthquake waveform data recorded over ~25 broadband seismic networks in the Himalayas, Tibet, and the Pamir-Hindu Kush to compute a 3-D shear wave velocity (V_s) model of the crust beneath the Kohistan and Ladakh arcs. The velocity model, with a lateral resolution of ~30 km, is derived using a Bayesian hierarchical trans-dimensional inversion of fundamental mode Rayleigh wave group velocity dispersion measurements. The result shows evidence of a uniform upper and middle crust ($V_s \sim 3.5\text{--}3.6$ km/s) underlain by an anomalous high-velocity layer (HVL) with $V_s > 4$ km/s at depths exceeding 40 km beneath the Kohistan arc, consistent with laboratory-derived crustal models showing its pre-collisional structures. The thickness of the HVL is maximum (>20 km) in southern Kohistan, which exposes the mafic and ultramafic arc crust. In contrast, the Ladakh arc, which has seismic structures similar to those in southern Tibet, is characterized by significantly low velocities ($V_s < 3.4$ km/s) in the middle crust (20–40 km depth) and a relatively thin HVL (~5–10 km) above a Moho depth, which mostly varies between 60 and 72 km. The contrasting velocity structure indicates that the Kohistan arc preserves a typical arc-like crust, whereas the Ladakh arc has undergone significant modifications since the India-Asia collision.

KEYWORDS

Kohistan-Ladakh arc, crustal structure, ambient noise tomography, lower crust, surface wave, island arc, trans-dimensional inversion

1 Introduction

Intra-oceanic island arcs are believed to have significantly contributed to the volume of continental crust since the Archean (Taylor and McLennan, 1985; Rudnick, 1995). The bulk composition of the continental crust is andesitic, whereas the island arc crust is basaltic, which is a well-known paradox. Therefore, if the continental crust is indeed formed by arc magmatism, significant modification of the island arc crust is required to transform the basaltic arc crust into the andesitic continental crust (Rudnick, 1995; Behn and Kelemen, 2006; Jagoutz and Schmidt, 2012; Jagoutz and Behn, 2013; Jagoutz and Kelemen, 2015). The Kohistan-Ladakh arc (KLA), sandwiched between the Karakoram in the north and the



western Himalayan syntaxis in the south (Figure 1), is recognized as a Mesozoic intra-oceanic island arc, preserving a complete arc section (Tahirikheli, 1979; Bard, 1983; Burg, 2011). Thus, knowledge of the nature of the crust beneath the KLA and its correlation with other modern island arcs and orogenic belts is critical to understanding the process of the formation of a juvenile continental crust from island arcs (Miller and Christensen, 1994; Jagoutz and Kelemen, 2015).

The crustal structure beneath the KLA is poorly investigated as compared to the rest of the Himalayas and Tibet, probably due to its

inaccessible and rugged terrain. Over the last few decades, several attempts have been made to understand the gross composition and seismic velocity structure, primarily using thermodynamic modelling and laboratory measurements of exposed rocks from the Kohistan arc (Chroston and Simmons, 1989; Miller and Christensen, 1994; Kono et al., 2009; Almqvist et al., 2013; Jagoutz and Behn, 2013). These studies reveal that the Kohistan arc represents a typical island arc crust characterized by a thin upper/mid crust overlying a very thick mafic high-velocity layer (HVL) with $V_p > 7$ km/s beyond 40 km depth. This unusually thick

mafic lower crust is interpreted as a density-unstable component of an arc crust that undergoes episodic modifications, probably via foundering, to create a typical continental crust of andesitic composition (Jagoutz and Behn, 2013; Jagoutz and Kelemen, 2015). However, the evidence of the arc-like preserved crust beneath the KLA has not yet been established using seismological observations, particularly because of the non-availability of broadband seismic stations, especially in Kohistan. The majority of the geophysical studies are confined to the eastern end of the Ladakh arc, which provides evidence of crust with low seismic velocities and partial melts (Rai et al., 2006, 2009; Caldwell et al., 2009). These results indicate strong crustal variability beneath the KLA that requires a high-resolution imaging of the region.

In this study, I compute a shear wave velocity (V_s) model of the crust beneath the KLA with a lateral resolution of ~ 30 km using a trans-dimensional Bayesian analysis (Bodin et al., 2012a; Hawkins and Sambridge, 2015) of a combination of ambient noise and earthquake data. Using the model, this study provides evidence of an arc-like preserved crust with a thick, high-velocity lower crust beneath the Kohistan and a modified arc crust with comparatively low velocities beneath the Ladakh arc that resembles the Karakoram and southern Tibet.

2 Geological context

The Kohistan-Ladakh terrain represents a fossil Cretaceous-Tertiary island arc complex that presumably formed over a north-dipping intra-oceanic subduction zone near the equator and, subsequently, was obducted between the colliding Indian and Eurasian plates at about 50 Ma (Tahirikheli, 1979; Bard, 1983; Jagoutz and Schmidt, 2012). The KLA is bounded by two suture zones (Figure 1). In the south, the Indus Suture Zone (ISZ), also referred to locally as the Main Mantle Thrust (MMT), separates the KLA from the western Himalaya. The Shyok Suture Zone (SSZ), or Main Karakoram Thrust (MKT), bounds the northern margin of the KLA and separates the Karakoram batholith in the north. The presence of these two suture zones, bounding the KLA, is interpreted as a result of two, almost parallel, north-dipping subduction zones (Supplementary Figure S1), one forming the KLA and another forming the Karakoram batholith, during the Early Cretaceous (Burg, 2011; Bouilhol et al., 2013; Jagoutz et al., 2015). The Nanga Parbat, sandwiched between the Kohistan arc in the west and the Ladakh arc in the east, is a fault-bounded, antiformal massif with the youngest exposed migmatites and granites (as young as 0.7 Ma) and the fastest exhumation rates up to ~ 13 mm/year (Zeitler et al., 1993; Crowley et al., 2009; Govin et al., 2020).

The Kohistan arc is broadly divided, from south to north, into three segments (Jagoutz and Schmidt, 2012). These include: 1) Southern Plutonic Complex: southernmost part of Kohistan, which exposes mafic to ultramafic arc lower crust formed during 120–85 Ma (Figure 1), 2) Chilas Complex: mafic to ultramafic intrusions representing mid-crustal arc rocks created by the arc rifting at around 85 Ma, and 3) Gilgit Complex: dominantly calc-alkaline batholith with inclusions of volcanic and sedimentary rocks, which exposes mid/upper arc crust and records a magmatic history from 120–50 Ma. Despite similarities with the Kohistan arc, the Ladakh batholith is characterized by a volumetrically large volcanic and

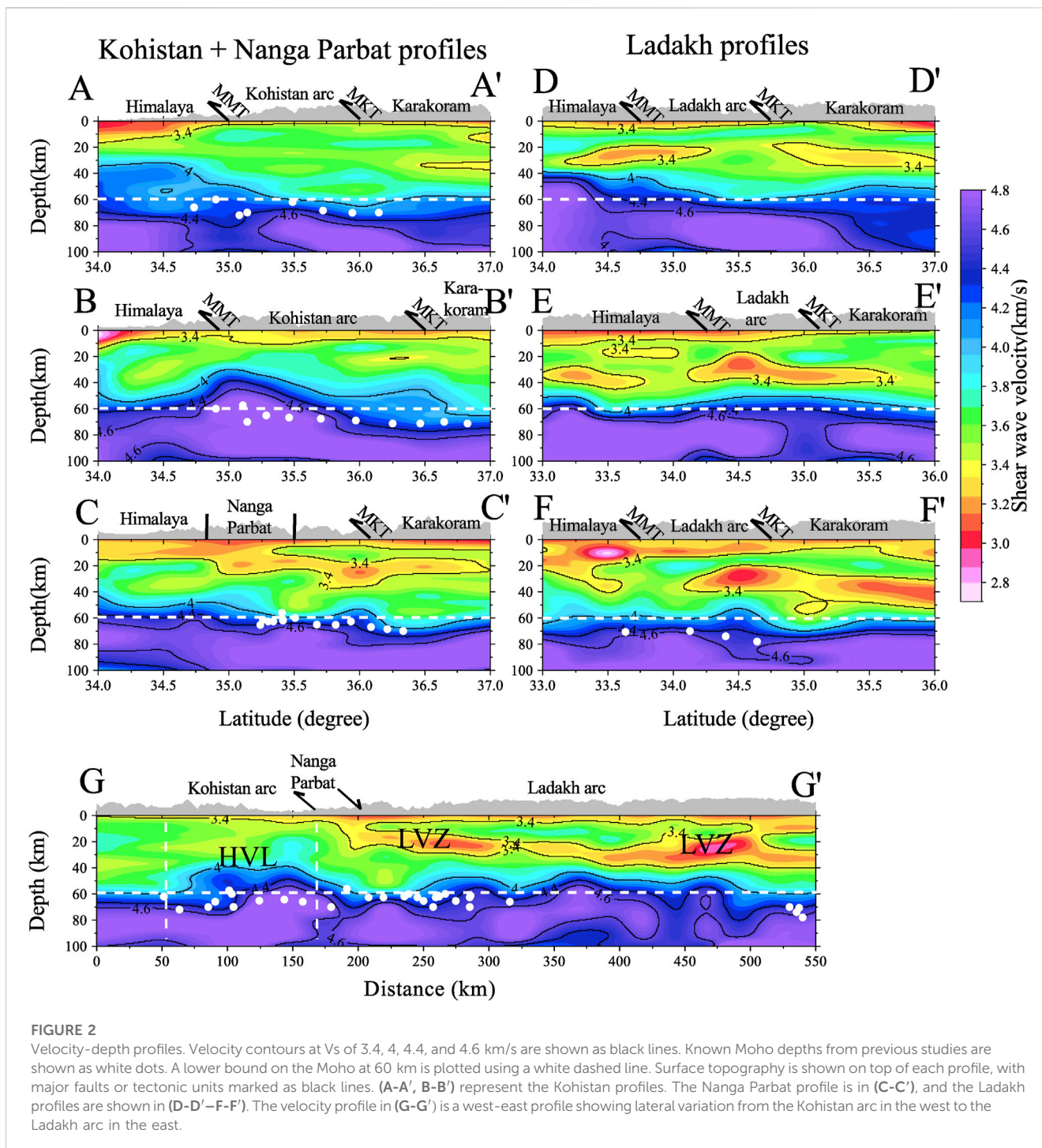
sedimentary unit with an increasing continental signature, which shows differences in tectonic processes eastward from the Kohistan (Rolland et al., 2000; Burg, 2011). The northeastern end of the Ladakh arc is bounded by the right-lateral Karakoram Fault (KKF).

3 Data and method

This study is built upon the previous work of Kumar et al. (2022) by reanalysing the data with a focus on the KLA. The dataset comes from ~ 530 broadband seismic stations located in the Pamir-Hindu Kush, western Tibet, western Himalaya, and adjoining areas. Fundamental mode Rayleigh wave group velocity measurements from period 5–60 s are obtained using analysis of ambient noise cross-correlations (Bensen et al., 2007; Schimmel et al., 2011) and earthquake waveforms recorded over the seismic stations (Supplementary Figure S2). The spatial resolution of group velocity dispersion is estimated by synthetic checkerboard tests (e.g., Rawlinson and Spakman, 2016). For this, input models with alternating positive and negative velocity anomalies of three different sizes ($0.2^\circ \times 0.2^\circ$, $0.3^\circ \times 0.3^\circ$, and $0.5^\circ \times 0.5^\circ$) are used. The recovered checkerboard models are presented in Supplementary Figures S3–S5, which show that the input models with sizes $0.3^\circ \times 0.3^\circ$ and $0.5^\circ \times 0.5^\circ$ are reasonably recovered, while the $0.2^\circ \times 0.2^\circ$ -sized model suffers from lateral smearing in the region encompassing the KLA and adjoining area.

Assuming an optimum lateral resolution of $0.3^\circ \times 0.3^\circ$ (~ 30 km), as discussed above, the study area is divided at a grid interval of $0.25^\circ \times 0.25^\circ$ and a two-step inversion scheme is adopted to compute the V_s model. First, a 2-D tomographic inversion is performed using the Bayesian trans-dimensional tree approach of Hawkins and Sambridge (2015), which provides group velocity maps in the period range of 5–60 s (Supplementary Figure S6). Subsequently, the group velocity dispersion at individual grid-nodes is inverted for the V_s -depth relation using a 1-D trans-dimensional Bayesian inversion of Bodin et al. (2012b). Finally, a 3-D shear wave velocity model is prepared by interpolating individual 1-D models. Detailed information about the data analysis and inversion scheme used in this study is described in Kumar et al. (2022), and a summary is provided in Supplementary Text S1.

Supplementary Figure S6 presents the group velocity maps at some representative periods (5–60 s) in terms of a perturbation from the regional mean. At shorter periods (5–20 s), which represent the upper crust, the group velocities within the KLA remain higher compared to sedimentary basins, e.g., Peshawar Basin, Shivalik sediments in the foothills of the western Himalaya, and the Tarim Basin, situated north of the KLA. At the intermediate period (30 s), sensitive to the middle crust, low-velocity zones (LVZs) appear beneath the Nanga Parbat and eastern Ladakh, which may indicate the presence of partial melts and/or aqueous fluids (e.g., Caldwell et al., 2009). For longer periods, i.e., more than 40 s, LVZs are observed primarily beneath the Nanga Parbat, the Karakoram, and eastern Ladakh. In contrast, the Kohistan arc, particularly its southern part, and western Ladakh (west of 76°E) show higher group velocities. The LVZs at these longer periods are possibly indicative of large crustal thickness and/or deep crustal melts beneath eastern Ladakh, i.e., the Baltoro batholith (Caldwell et al., 2009). To constrain the depth variation of shear wave



velocities, the dispersion data at multiple periods is inverted for the V_s -depth relation and discussed in the following sections.

4 Results

4.1 Regional shear wave velocity model

Supplementary Figure S7 presents the constant-depth horizontal slices of V_s maps. In the upper crust (~10 km), the KLA and the

Karakoram region exhibit high velocities, whereas the Peshawar Basin in the southwest of the KLA shows LVZs due to its sediment thickness. In the depth range of 20–30 km, LVZs are observed in Nanga Parbat and Ladakh, probably indicating melts/fluids (Caldwell et al., 2009). A small LVZ, just south of Kohistan at 20 km depth (Supplementary Figure S7B), may indicate a continuation of the LVZ in the Peshawar Basin (e.g., Li and Mashele, 2009) and/or melts/fluids. An interesting abnormal feature is present at depths ≥ 40 km (at least down to 60 km), where a high-velocity zone (HVZ) is observed beneath the

southern part of the Kohistan arc (Chilas + Southern Plutonic Complex, [Figure 1](#)). In contrast, the regions surrounding eastern Ladakh, the Karakoram batholith, and western Tibet are characterized by LVZs, possibly due to their large crustal thickness ([Rai et al., 2006](#)). At deeper depths (70–80 km), the LVZs are mainly observed in western Tibet and the Karakoram region, indicating the northward crustal thickening due to the underthrusting Indian crust. To further explore the nature of HVZs in the Kohistan arc and the LVZs in Ladakh and Nanga Parbat, several north-south and east-west trending velocity-depth sections are presented and discussed below.

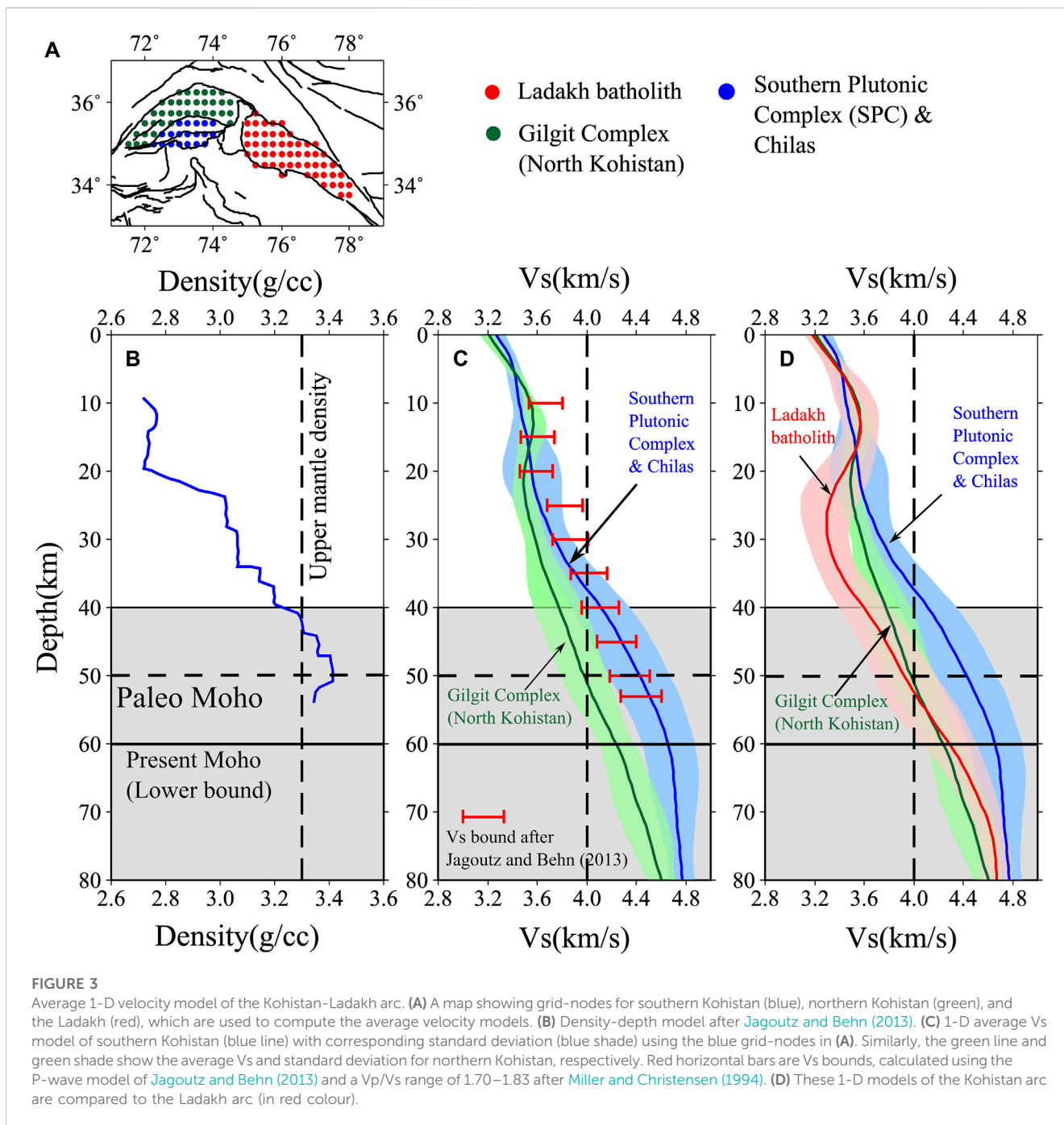
4.2 Shear wave velocity-depth sections

A total of 12 north-south trending velocity-depth profiles, which cross-cut the KLA, and three east-west trending profiles roughly parallel to the strike of the KLA are presented in [Figure 2](#) and [Supplementary Figures S8, S9](#). To interpret these velocity profiles, a knowledge of the variation of crustal thickness in the KLA is required. The inversion of the surface wave suffers from a strong trade-off between the Moho and shear wave velocities above and below the Moho ([Lebedev et al., 2013](#)). Furthermore, the role of geothermal gradient on shear wave velocities around the Moho needs to be carefully examined ([Diaferia and Cammarano, 2017](#)). Therefore, a detailed discussion about the crust-mantle trade-offs, uncertainty in estimated velocity models, and their comparison with published models is presented in [Supplementary Text S2](#) and [Supplementary Figures S15–S19](#). Based on the previously published Moho depths, shown as white dots in velocity profiles ([Belousov et al., 1980](#); [Verma and Prasad, 1987](#); [Rai et al., 2006](#); [Oreshin et al., 2008](#); [Priestley et al., 2019](#); [Schneider et al., 2019](#)) and this study's velocity model, the crustal thickness in the KLA varies between 60 and 72 km, except in the eastern Ladakh, where it is ~75–80 km. The base of the Moho is identified at $V_s > 4.4$ km/s ([Supplementary Figure S19](#)), consistent with previous studies in the Himalayas and southern Tibet ([Rai et al., 2006](#); [Pei et al., 2011](#); [Hazari et al., 2017](#)). In this study, a lower bound of 60 km for the Moho depth (white dashed lines in velocity profiles) is adopted for further interpretation. A $V_s > 4$ km/s above the Moho is termed a high-velocity layer (HVL) or a 7x layer ($V_p > 7$ km/s; [Christensen and Mooney, 1995](#); [Schulte-Pelkum et al., 2017](#)). The HVL is formed by various mechanisms, e.g., magmatic addition to the lower crust ([Supplementary Figure S1](#)) and/or lower crustal eclogitization ([Sapin and Hirn, 1997](#); [Nábělek et al., 2009](#)). In the context of the Himalayas and Tibet, the HVL is traditionally interpreted as the underthrusting mafic lower crust of the Indian plate ([Schulte-Pelkum et al., 2005](#); [Nábělek et al., 2009](#)). In the mid-crustal depth (20–40 km), $V_s < 3.4$ km/s can be attributed to the presence of melts or aqueous fluids ([Yang et al., 2012](#)).

Upper-crustal LVZs, primarily south of the MMT, at depths of 0–20 km ($V_s < 3.4$ km/s), are observed in almost all N-S profiles, which indicates the contribution of sediment thickness in the western Himalaya. The first two profiles (A-A', B-B') in [Figure 2](#) and the first three profiles (I-I' to III-III') in [Supplementary Figure S8](#) are cross-cutting the Kohistan arc. They reveal a simple crust beneath the Kohistan arc with an

average V_s of 3.5–3.6 km/s. However, an unusually thick, at least 20 km, HVL is observed in the depth range of 40–60 km in profile B-B' ([Figure 2](#)) and profile II-II' ([Supplementary Figure S8](#)). The thickness of this HVL is most significant in southern Kohistan, where the mafic/ultramafic arc lower crust is exposed ([Figure 1](#)). The velocity profiles presented in [Figures 2C-C'–F-F'](#) and [Supplementary Figures S8IV-IV'–VI-VI'](#) cross-cut the Nanga Parbat, Ladakh, the Karakoram, and the western Himalaya. Two primary observations can be made from these profiles. First, mid-crustal LVZs ($V_s < 3.4$ km) at depths exceeding 20 km. The maximum depth of these LVZs increases from ~20 km in Nanga Parbat (profile C-C', [Figure 2](#)) to ~50 km in eastern Ladakh (profile F-F' in [Figure 2](#) and profile VI-VI' in [Supplementary Figure S8](#)). Second, no unusually thick HVL, as observed in the Kohistan arc, is observed in the Ladakh and Nanga Parbat regions. The mid-crustal LVZs are possibly indicating the presence of melts and/or aqueous fluids released due to dehydration reaction as the Indian crust underthrusts ([Caldwell et al., 2009](#); [Yang et al., 2012](#); [Li et al., 2018](#); [Kumar et al., 2022](#)).

The observation of contrasting crustal structure, as discussed above, is summarized in three along-arc profiles in [Figure 2](#) (profile G-G') and [Supplementary Figure S9](#). A thick underplated lower crust (i.e., HVL), with a minimum thickness of 20 km, at depths >40 km and a uniform upper/mid crust with no evidence of mid-crustal LVZs are imaged beneath the Kohistan arc. Beneath the Ladakh arc, the HVL is relatively thin. Considering that a $V_s > 4.4$ km/s marks the base of the Moho in the Ladakh area, as discussed in [Supplementary Text S2](#), the width between the contours for V_s 4 and 4.4 km/s varies around 5–10 km ([Figure 2](#), profile G-G'). A similar thickness of the lowermost crust is also observed in the Himalayas and southern Tibet ([Nábělek et al., 2009](#); [Kumar et al., 2022](#)), which indicates the underthrusting Indian lower crust. A small packet of LVZ (at ~20 km depth) beneath the Kohistan arc, in the southernmost velocity profile (VII-VII' in [Supplementary Figure S9](#)), is interpreted as a possible extension of the Peshawar Basin (see profile II-II' in [Supplementary Figure S8](#)). The thick upper crustal low velocities (up to 20 km depth) in the Peshawar Basin are also observed by [Li and Mashele \(2009\)](#). Alternatively, it can also represent melts/fluid above the Main Himalayan Thrust ([Caldwell et al., 2013](#)), a boundary separating the Himalayan crust and the underthrusting Indian crust. The mid-crustal LVZs beneath Ladakh appear continuous in the southern profiles (G-G' in [Figure 2](#) and VII-VII' in [Supplementary Figure S9](#)). However, the LVZs get disconnected further north (profile VIII-VIII' in [Supplementary Figure S9](#)). Note that the dominant low velocities ($V_s \leq 3.2$ km/s) are observed at two places: one beneath eastern Ladakh, and the other ~50 km east of the Nanga Parbat Massif. I argue that these LVZs are possibly disconnected, consistent with the earlier observation of disconnected conductive zones in the Nanga Parbat area ([Park and Mackie, 2000](#)). The mid-crustal LVZ, 50 km east of the Nanga Parbat, possibly indicates an isolated source for the westward flow of mid-crustal melts, same as suggested by [Park and Mackie \(2000\)](#), and its exhumation onto the surface of the Nanga Parbat, which may explain the cause of the high exhumation rate ([Guevara et al., 2022](#)). The linkage between the deep crustal reworking and the surface processes related to the

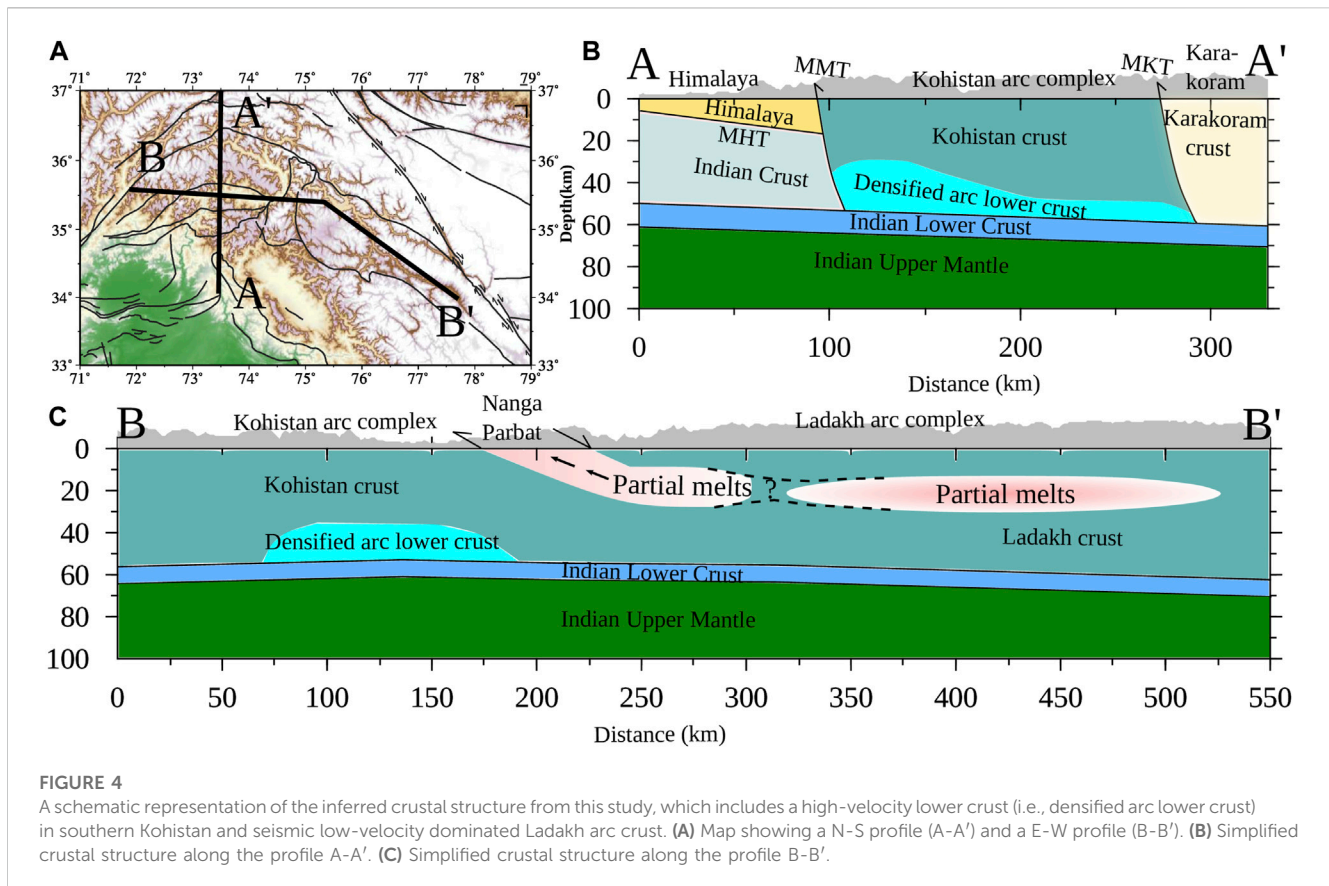


evolution of the Nanga Parbat Massif calls for in-depth investigations in the future. In the section below, the implication of the contrasting velocity structures observed beneath the KLA is discussed.

5 Discussion

The seismic structure of island arcs provides along-strike variability in the arc crust, which provides evidence of arc modifications leading to the formation of modern continental

crust [reviewed in Rudnick (1995) and Calvert (2011)]. Modern island arcs are typically characterized by a high-velocity lower crust, indicating the predominant mafic nature of the arc crust as compared to a more felsic continental crust (Calvert, 2011). Chroston and Simmons (1989) and Miller and Christensen (1994) reconstructed the seismic structure of the Kohistan arc before its obduction onto the Indian plate using geothermobarometry and thermodynamic modelling of exposed rock samples. Their studies demonstrated that Kohistan is representative of a typical arc-like crust with a thin upper and middle crust overlying a thick HVL ($V_p \sim 6.8\text{--}7.8$ km/s) in the lower



crust. Beyond 40 km depth, these studies predict strong inflection in V_p (>7.0 km/s), V_s (>4.0 km/s), and density (>3.3 g/cc). The crustal thickness was estimated to be around 50 km. Jagoutz and Behn (2013), using a large sample of exposed rocks from Kohistan, reconstructed a seismic structure showing a negatively buoyant lower crust at depths exceeding 40 km. Further evidence of the densified arc crust beneath the Kohistan comes from gravity measurements by Verma and Prasad (1987) showing a locally high Bouguer anomaly (Supplementary Figure S17B) in southern Kohistan, which was interpreted as the result of high-density shallow crustal intrusions from the deep crust/upper mantle. Based on these studies, it is evident that the Kohistan arc represents a well-preserved paleo-arc crust. A surface wave study by Hanna and Weeraratne (2013) provided an average 1-D velocity of Nanga Parbat and the KLA, but could not image the lateral variability in the interior of the KLA because of low ray coverage away from the Nanga Parbat Massif. On the other hand, several studies in the Ladakh arc show evidence of the contrasting structure of the crust, dominated by low seismic velocities, possibly due to melting (Caldwell et al., 2009; Rai et al., 2009).

The crustal velocity model presented in this study, which has a lateral resolution of ~ 30 km, provides a unique opportunity to investigate the crustal variability within the KLA. Based on the contrasting velocity structure beneath the KLA, discussed in the earlier section, the area can be divided into major blocks, and their average velocities can be compared to previously computed models. In Figure 3, average 1-D V_s models are provided for different regions

of the KLA and compared with the laboratory-derived model of Jagoutz and Behn (2013). The Kohistan arc is divided into two blocks: 1) southern Kohistan (Chilas + Southern Plutonic Complex), which exposes the mafic/ultra-mafic lower crustal rocks (blue dots in Figure 3A), and 2) northern Kohistan, which includes the Gilgit complex, dominated by the calc-alkaline batholith and sediments (green dots in Figure 3A). The Ladakh batholith is presented in red dots. These colored dots in Figure 3A represent grid-nodes of the velocity model within the KLA. The density-depth relation of the Kohistan arc, before its obduction on the Indian plate (Jagoutz and Behn, 2013), is shown in Figure 3B, which shows the density-unstable lower crust at depths >40 km. The 1-D average V_s beneath the Kohistan arc (Figure 3C) shows a uniform upper/middle crust of $V_s \sim 3.5$ – 3.6 km/s, and a thick HVL (>20 km) in the lower crust ($V_s > 4.0$ km/s) at depths >40 km in the southern Kohistan, consistent with the density-unstable lower crust. The lower crustal velocities in northern Kohistan are significantly lower as compared to southern Kohistan, indicating northward thinning and/or the absence of the anomalous high-density lower crust. Note that the observation of the anomalously thick densified arc lower crust beneath southern Kohistan matches well with the locally observed high Bouguer anomaly (Verma and Prasad, 1987), as discussed earlier. Additionally, the distribution of exposed rock properties on the surface of the Kohistan arc shows a similar pattern. In southern Kohistan, mafic/ultramafic arc lower crustal rocks are exposed, whereas the upper crustal

rocks, e.g., calc-alkaline batholith, are exposed in northern Kohistan (Figure 1). This correlation between the deep structure and the exposed rock properties in the Kohistan arc possibly indicates the southward thrusting of the arc's lower crustal rocks over a north-dipping Indian crust during the India-Asia collision, which resulted in the obduction of mafic/ultramafic crust in the southern Kohistan. Using the V_p/V_s range of 1.70–1.83 for the Kohistan arc (Miller and Christensen, 1994) and the P-wave model of Jagoutz and Behn (2013), the possible range of shear wave velocities for the pre-collisional arc crust is shown as red horizontal bars in Figure 3C. This study's average crustal velocity values in southern Kohistan are remarkably similar to those obtained by laboratory measurements. At depths between 20 and 30 km, the model of Jagoutz and Behn (2013) shows higher velocities, possibly due to the presence of an ultramafic horizon within a layered mafic intrusion of the order of 1 km thickness, which is difficult to resolve in seismic experiments (see Miller and Christensen, 1994). These results indicate that a typical arc-like crust is preserved in the Kohistan arc.

The average velocity of the Ladakh arc is presented in Figure 3D. The mid-crustal (at 20–40 km depth) velocities are reduced by 10%–15% as compared to the Kohistan arc, possibly indicating the effect of the Baltoro granite melting (Caldwell et al., 2009). In the Ladakh arc, the HVL ($V_s > 4$ km/s above Moho) is relatively thin (~10 km) beyond 50 km depth. The velocity structure in the Ladakh arc is comparable to that in southern Tibet (Yang et al., 2012). The thin HVL above the Moho beneath the Ladakh arc represents the underthrusting Indian lower crust that reaches up to varying latitudes in the Pamir and Tibet (Kumar et al., 2022). Thus, the unusually thick HVL beneath the Kohistan arc must include a density-unstable arc lower crustal root, as predicted by previous studies, overlying the underthrusting Indian lower crust.

In summary, the velocity structure beneath the Kohistan arc is comparable to the pre-collisional structure derived by laboratory measurements, which indicates that the Kohistan arc has a well-preserved arc-like crust. The anomalously dense lower crust in southern Kohistan possibly represents the density-unstable arc root, typically found in modern arcs. With time, this densified root becomes heavier than the underlying upper mantle and may undergo episodic foundering, ultimately resulting in an andesitic continental crust (Jagoutz and Behn, 2013; Jagoutz and Kelemen, 2015). In contrast, the Ladakh arc, which behaves more like southern Tibet, has undergone significant modifications after the India-Asia collision. This contrasting crustal structure of the KLA is presented in a schematic diagram in Figure 4, which highlights the variability in the nature of tectonic processes in the KLA, as envisioned by Burg (2006).

6 Conclusion

A 3-D shear wave velocity model of crust, with a lateral resolution of ~30 km, beneath the Kohistan-Ladakh arc is derived using ambient noise and earthquake waveform analysis based on Bayesian trans-dimensional inversion. The results are summarized in Figures 3, 4 and the major findings are listed below:

- 1) A uniform upper and middle crust of $V_s \sim 3.5$ – 3.6 km/s and an anomalous high-velocity lower crust ($V_s > 4$ km/s) at depths exceeding 40 km are observed beneath the Kohistan arc.
- 2) The thickness of the high-velocity lower crust is maximum (>20 km) in southern Kohistan where mafic and ultramafic arc crust is exposed.
- 3) The average velocity model of the Kohistan arc is comparable to laboratory-derived models providing pre-collisional structures.
- 4) In contrast, the Ladakh arc is characterized by a low-velocity middle crust ($V_s < 3.4$ km/s at 20–40 km depth) and a relatively thin (5–10 km) high-velocity lower crust, similar to those in southern Tibet.
- 5) The Kohistan arc preserves a typical arc-like structure, while the Ladakh arc was significantly modified after the India-Asia collision.

Data availability statement

The datasets presented in this study can be found in online repositories. The names of the repository/repositories and accession number(s) can be found below: <https://ds.iris.edu/ds/nodes/dmc/>, <https://geofon.gfz-potsdam.de/waveform/archive/>, <https://doi.org/10.1029/2021JB022574>.

Author contributions

VK: Conceptualization, Data curation, Formal Analysis, Methodology, Software, Writing—original draft, Writing—review and editing.

Funding

The author(s) declare financial support was received for the research, authorship, and/or publication of this article. The research funding for this study is obtained from the Department of Atomic Energy, India. VK was supported by the Research Associateship from the Department of Atomic Energy, India (grant no. 1003/2/2021/RRF/R&D-II/5959).

Acknowledgments

The author is extremely thankful to his project guide Prof. Shyam S. Rai for guiding and providing the necessary support for the completion of this manuscript. The author also acknowledges support from Dr. Rhys Hawkins and Dr. Thomas Bodin, who contributed to the trans-dimensional inversion analysis. Critical comments from the reviewers helped improve the manuscript. Seismic broadband data, used in this study, are taken from IRIS DMC (<https://ds.iris.edu/ds/nodes/dmc/>), GEOFON (<https://geofon.gfz-potsdam.de/waveform/archive/>), CSIR-4PI, Wadia Institute of Himalayan Geology (WIGH), and CSIR-National Geophysical Research Institute (NGRI), and are duly acknowledged. All the data processing is performed on the Seismic Analysis Code (<https://ds.iris.edu/ds/nodes/dmc/forms/sac/>) and figures are prepared using the Generic Mapping Tool (<https://www.generic-mapping-tools.org>).

Conflict of interest

The author declares that the research was conducted in the absence of any commercial or financial relationships that could be construed as a potential conflict of interest.

Publisher's note

All claims expressed in this article are solely those of the authors and do not necessarily represent those of their affiliated

organizations, or those of the publisher, the editors and the reviewers. Any product that may be evaluated in this article, or claim that may be made by its manufacturer, is not guaranteed or endorsed by the publisher.

Supplementary material

The Supplementary Material for this article can be found online at: <https://www.frontiersin.org/articles/10.3389/feart.2023.1264415/full#supplementary-material>

References

- Almqvist, B. S. G., Burg, J.-P., Berger, J., and Burlini, L. (2013). Seismic properties of the Kohistan oceanic arc root: insights from laboratory measurements and thermodynamic modeling. *Geochem. Geophys. Geosystems* 14, 1819–1841. doi:10.1002/ggge.20125
- Bard, J. P. (1983). Metamorphism of an obducted island arc: example of the Kohistan sequence (Pakistan) in the Himalayan collided range. *Earth Planet Sci. Lett.* 65, 133–144. doi:10.1016/0012-821X(83)90195-4
- Behn, M. D., and Kelemen, P. B. (2006). Stability of arc lower crust: insights from the Talkeetna arc section, south central Alaska, and the seismic structure of modern arcs. *J. Geophys. Res. Solid Earth* 111, n/a. doi:10.1029/2006JB004327
- Belousov, V. V., Belyaevsky, N. A., Borisov, A. A., Volvovsky, B. S., Volkovsky, I. S., Resvoy, D. P., et al. (1980). Structure of the lithosphere along the deep seismic sounding profile: tien Shan—pamirs—Karakorum—Himalayas. *Tectonophysics* 70, 193–221. doi:10.1016/0040-1951(80)90279-6
- Bensen, G. D., Ritzwoller, M. H., Barmin, M. P., Levshin, A. L., Lin, F., Moschetti, M. P., et al. (2007). Processing seismic ambient noise data to obtain reliable broad-band surface wave dispersion measurements. *Geophys J. Int.* 169, 1239–1260. doi:10.1111/j.1365-246X.2007.03374.x
- Bodin, T., Sambridge, M., Rawlinson, N., and Arroucau, P. (2012a). Transdimensional tomography with unknown data noise. *Geophys J. Int.* 189, 1536–1556. doi:10.1111/j.1365-246X.2012.05414.x
- Bodin, T., Sambridge, M., Tkalcic, H., Arroucau, P., Gallagher, K., and Rawlinson, N. (2012b). Transdimensional inversion of receiver functions and surface wave dispersion. *J. Geophys. Res. Solid Earth* 117, n/a. doi:10.1029/2011JB008560
- Bouilhol, P., Jagoutz, O., Hanchar, J. M., and Dudas, F. O. (2013). Dating the India–Eurasia collision through arc magmatic records. *Earth Planet Sci. Lett.* 366, 163–175. doi:10.1016/j.epsl.2013.01.023
- Burg, J.-P. (2006). Two orogenic systems and a transform-transfer fault in the Himalayas: evidence and consequences. *Earth Sci. Front.* 13.
- Burg, J.-P. (2011). “The asia–kohistan–India collision: review and discussion,” in *Arc-continent collision*, 279–309. doi:10.1007/978-3-540-88558-0_10
- Caldwell, W. B., Klemperer, S. L., Lawrence, J. F., Rai, S. S., and Ashish, (2013). Characterizing the Main Himalayan Thrust in the garhwal Himalaya, India with receiver function CCP stacking. *Earth Planet Sci. Lett.* 367, 15–27. doi:10.1016/j.epsl.2013.02.009
- Caldwell, W. B., Klemperer, S. L., Rai, S. S., and Lawrence, J. F. (2009). Partial melt in the upper-middle crust of the northwest Himalaya revealed by Rayleigh wave dispersion. *Tectonophysics* 477, 58–65. doi:10.1016/j.tecto.2009.01.013
- Calvert, A. J. (2011). “The seismic structure of Island Arc crust,” in *Arc-continent collision*, 87–119. doi:10.1007/978-3-540-88558-0_4
- Christensen, N. L., and Mooney, W. D. (1995). Seismic velocity structure and composition of the continental crust: a global view. *J. Geophys. Res. Solid Earth* 100, 9761–9788. doi:10.1029/95JB00259
- Chroston, P. N., and Simmons, G. (1989). Seismic velocities from the kohistan volcanic arc, northern Pakistan. *J. Geol. Soc. Lond.* 146, 971–979. doi:10.1144/gsjgs.146.6.0971
- Crowley, J. L., Waters, D. J., Searle, M. P., and Bowring, S. A. (2009). Pleistocene melting and rapid exhumation of the Nanga Parbat massif, Pakistan: age and P–T conditions of accessory mineral growth in migmatite and leucogranite. *Earth Planet Sci. Lett.* 288, 408–420. doi:10.1016/j.epsl.2009.09.044
- Diaferia, G., and Cammarano, F. (2017). Seismic signature of the continental crust: what thermodynamics says. An example from the Italian peninsula. *Tectonics* 36, 3192–3208. doi:10.1002/2016TC004405
- Govin, G., van der Beek, P., Najman, Y., Millar, I., Gemignani, L., Huyghe, P., et al. (2020). Early onset and late acceleration of rapid exhumation in the Namche Barwa syntaxis, eastern Himalaya. *Geology* 48, 1139–1143. doi:10.1130/G47720.1
- Guevara, V. E., Smye, A. J., Caddick, M. J., Searle, M. P., Olsen, T., Whalen, L., et al. (2022). A modern pulse of ultrafast exhumation and diachronous crustal melting in the Nanga Parbat Massif. *Sci. Adv.* 8, eabm2689. doi:10.1126/sciadv.abm2689
- Hanna, A. C., and Weeraratne, D. S. (2013). Surface wave velocity structure of the western Himalayan syntaxis. *Geophys J. Int.* 194, 1866–1877. doi:10.1093/gji/ggt203
- Hawkins, R., and Sambridge, M. (2015). Geophysical imaging using trans-dimensional trees. *Geophys J. Int.* 203, 972–1000. doi:10.1093/gji/ggv326
- Hazarika, D., Wadhawan, M., Paul, A., Kumar, N., and Borah, K. (2017). Geometry of the Main Himalayan Thrust and Moho beneath satluj valley, northwest Himalaya: constraints from receiver function analysis. *J. Geophys. Res. Solid Earth* 122, 2929–2945. doi:10.1002/2016JB013783
- Jagoutz, O., and Behn, M. D. (2013). Foundering of lower island-arc crust as an explanation for the origin of the continental Moho. *Nature* 504, 131–134. doi:10.1038/nature12758
- Jagoutz, O., and Kelemen, P. B. (2015). Role of arc processes in the formation of continental crust. *Annu. Rev. Earth Planet Sci.* 43, 363–404. doi:10.1146/annurev-earth-040809-152345
- Jagoutz, O., Royden, L., Holt, A. F., and Becker, T. W. (2015). Anomalous fast convergence of India and Eurasia caused by double subduction. *Nat. Geosci.* 8, 475–478. doi:10.1038/ngeo2418
- Jagoutz, O., and Schmidt, M. W. (2012). The formation and bulk composition of modern juvenile continental crust: the Kohistan arc. *Chem. Geol.* 298–299, 79–96. doi:10.1016/j.chemgeo.2011.10.022
- Kono, Y., Ishikawa, M., Harigane, Y., Michibayashi, K., and Arima, M. (2009). P- and S-wave velocities of the lowermost crustal rocks from the Kohistan arc: implications for seismic Moho discontinuity attributed to abundant garnet. *Tectonophysics* 467, 44–54. doi:10.1016/j.tecto.2008.12.010
- Kumar, V., Rai, S. S., Hawkins, R., and Bodin, T. (2022). Seismic imaging of crust beneath the western tibet-pamir and western Himalaya using ambient noise and earthquake data. *J. Geophys. Res. Solid Earth* 127. doi:10.1029/2021JB022574
- Lebedev, S., Adam, J. M.-C., and Meier, T. (2013). Mapping the Moho with seismic surface waves: a review, resolution analysis, and recommended inversion strategies. *Tectonophysics* 609, 377–394. doi:10.1016/j.tecto.2012.12.030
- Li, A., and Mashele, B. (2009). Crustal structure in the Pakistan Himalaya from teleseismic receiver functions. *Geochem. Geophys. Geosystems* 10, n/a. doi:10.1029/2009GC002700
- Li, W., Chen, Y., Yuan, X., Schurr, B., Mechie, J., Oimahmadov, I., et al. (2018). Continental lithospheric subduction and intermediate-depth seismicity: constraints from S-wave velocity structures in the Pamir and Hindu Kush. *Earth Planet Sci. Lett.* 482, 478–489. doi:10.1016/j.epsl.2017.11.031
- Miller, D. J., and Christensen, N. L. (1994). Seismic signature and geochemistry of an island arc: a multidisciplinary study of the Kohistan accreted terrane, northern Pakistan. *J. Geophys. Res. Solid Earth* 99, 11623–11642. doi:10.1029/94JB00059
- Nábělek, J., Hetényi, G., Vergne, J., Sapkota, S., Kafle, B., Jiang, M., et al. (2009). Underplating in the Himalaya–Tibet collision zone revealed by the hi-CLIMB experiment. *Sci.* (1979) 325, 1371–1374. doi:10.1126/science.1167719
- Oreshin, S., Kiselev, S., Vinnik, L., Surya Prakasam, K., Rai, S. S., Makeyeva, L., et al. (2008). Crust and mantle beneath western Himalaya, Ladakh and western Tibet from integrated seismic data. *Earth Planet Sci. Lett.* 271, 75–87. doi:10.1016/j.epsl.2008.03.048
- Park, S. K., and Mackie, R. L. (2000). Resistive (dry?) lower crust in an active orogen, Nanga Parbat, northern Pakistan. *Tectonophysics* 316, 359–380. doi:10.1016/S0040-1951(99)00264-4

- Pei, S., Sun, Y., and Toksöz, M. N. (2011). Tomographic Pn and Sn velocity beneath the continental collision zone from Alps to Himalaya. *J. Geophys. Res.* 116, B10311. doi:10.1029/2010JB007845
- Priestley, K., Ho, T., and Mitra, S. (2019). The crustal structure of the Himalaya: a synthesis. *Geol. Soc. Lond. Spec. Publ.* 483, 483–516. doi:10.1144/SP483-2018-127
- Rai, S. S., Ashish, , Padhi, A., and Sarma, P. R. (2009). High crustal seismic attenuation in Ladakh-Karakoram. *Bull. Seismol. Soc. Am.* 99, 407–415. doi:10.1785/0120070261
- Rai, S. S., Priestley, K., Gaur, V. K., Mitra, S., Singh, M. P., and Searle, M. (2006). Configuration of the Indian Moho beneath the NW Himalaya and Ladakh. *Geophys. Res. Lett.* 33, L15308. doi:10.1029/2006GL026076
- Rawlinson, N., and Spakman, W. (2016). On the use of sensitivity tests in seismic tomography. *Geophys. J. Int.* 205, 1221–1243. doi:10.1093/gji/ggw084
- Rolland, Y., Pècher, A., and Picard, C. (2000). Middle Cretaceous back-arc formation and arc evolution along the Asian margin: the Shyok suture zone in northern Ladakh (NW Himalaya). *Tectonophysics* 325, 145–173. doi:10.1016/S0040-1951(00)00135-9
- Rudnick, R. L. (1995). Making continental crust. *Nature* 378, 571–578. doi:10.1038/378571a0
- Sapin, M., and Hirn, A. (1997). Seismic structure and evidence for eclogitization during the Himalayan convergence. *Tectonophysics* 273, 1–16. doi:10.1016/S0040-1951(96)00285-5
- Schimmel, M., Stutzmann, E., and Gallart, J. (2011). Using instantaneous phase coherence for signal extraction from ambient noise data at a local to a global scale. *Geophys. J. Int.* 184, 494–506. doi:10.1111/j.1365-246X.2010.04861.x
- Schneider, F. M., Yuan, X., Schurr, B., Mechie, J., Sippl, C., Kufner, S. K., et al. (2019). The crust in the Pamir: insights from receiver functions. *J. Geophys. Res. Solid Earth* 124, 9313–9331. doi:10.1029/2019JB017765
- Schulte-Pelkum, V., Mahan, K. H., Shen, W., and Stachnik, J. C. (2017). The distribution and composition of high-velocity lower crust across the continental U.S.: comparison of seismic and xenolith data and implications for lithospheric dynamics and history. *Tectonics* 36, 1455–1496. doi:10.1002/2017TC004480
- Schulte-Pelkum, V., Monsalve, G., Sheehan, A., Pandey, M. R., Sapkota, S., Bilham, R., et al. (2005). Imaging the Indian subcontinent beneath the Himalaya. *Nature* 435, 1222–1225. doi:10.1038/nature03678
- Tahirkehi, R. K. (1979). Geology of Kohistan and adjoining Eurasian and Indo-Pakistan continents, Pakistan. *Geol. Bull. Univ. Peshawar* 11, 1–30.
- Taylor, S. R., and McLennan, S. M. (1985). *The continental crust: its composition and evolution*. United States.
- Verma, R. K., and Prasad, K. A. V. L. (1987). Analysis of gravity fields in the northwestern Himalayas and Kohistan region using deep seismic sounding data. *Geophys. J. Int.* 91, 869–889. doi:10.1111/j.1365-246X.1987.tb01672.x
- Yang, Y., Ritzwoller, M. H., Zheng, Y., Shen, W., Levshin, A. L., and Xie, Z. (2012). A synoptic view of the distribution and connectivity of the mid-crustal low velocity zone beneath Tibet. *J. Geophys. Res. Solid Earth* 117, n/a. doi:10.1029/2011JB008810
- Zeitler, P. K., Chamberlain, C. P., and Smith, H. A. (1993). Synchronous anatexis, metamorphism, and rapid denudation at Nanga Parbat (Pakistan Himalaya). *Geology* 21, 347. doi:10.1130/0091-7613(1993)021<0347:SAMARD>2.3.CO;2